PAPER REF: 3935

# MODELLING THE PULLOUT OF HOOKED STEEL FIBERS FROM CEMENTITIOUS MATRIX

**Edmunds Zīle[1(*)], Olga Zīle[1]**

[1]Institute of Polymer Mechanics of the University of Latvia, Riga, Latvia
[(*)]*Email:* edmunds.zile@gmail.com

## ABSTRACT

A simple model to predict the influence of fiber geometry on the pullout of mechanically deformed steel fibers from cementitious matrix is proposed. During the pullout the mechanically deformed fiber is subjected to repetitive bending and unbending which causes an increase of the tension in the fiber. This increase of the tension depends on the amount of plastic work needed to straighten the fiber during pullout. The model input parameters are mechanical and geometrical properties of mechanically deformed fibers. Model predictions were compared to the experimental results on the hooked-end fiber pullout and good agreement was observed.

**Keywords:** Pull-Out Strength, Tensile Properties, Fiber Reinforcement

## INTRODUCTION

Concrete is a brittle material with low ductility. The tensile strain capacity of the concrete is low, and the tensile strength is only about 5% to 10% of its compressive strength. To improve the above mentioned properties of the concrete, FRC (fiber reinforced concrete) has been developed, which is defined as concrete containing dispersed randomly oriented short fibers. The main role of dispersed fibers is to control the crack opening and propagation by bridging the crack faces and providing resistance to crack opening whichever directions the cracks form. The addition of fibers greatly enhances the post-peak structural ductility, a quantity valued by the engineers for safety reasons. Steel fiber is the most common type of fiber used to reinforce concrete.

The bridging action provided by the fibers strongly depends on the pullout mechanism. A pullout test of a single fiber embedded in cementitious matrix can be used to assess the effectiveness of the fiber. Although pullout of straight steel fibers have been extensively analyzed by many researchers (Alwan, 1991; Naaman, 1991a, 1991b; Geng, 1997; Leung, 1999; Laranjeira, 2009; Lee, 2010), experiments have shown that in improving the pullout resistance, mechanically deformed fibers are more effective than straight fibers (Banthia, 1994; Robins, 2002; Cunha, 2010) due to mechanical anchorage created by the deformed shape of the fiber. While the fiber/matrix debonding and frictional sliding are the two main mechanisms controlling the pullout of straight fibers, additional mechanism due to fiber straightening during pullout must be taken into account for mechanically deformed fibers, which introduces additional complexity on the pullout response.

There are few attempts to model the effect of fiber geometry on pullout of steel fibers (Chanvillard, 1999; Alwan, 1999; Sujivorakul, 2000; Georgiadi-Stefanidi, 2010; Laranjeira, 2010). In (Chanvillard, 1999) a model was proposed which accounts for fiber deformation during pullout requiring a numerical integration procedure to obtain the pullout load – displacement curve. In (Alwan, 1999) frictional pulley model to predict the pullout force of

hooked-end steel fibers was developed. In (Sujivorakul, 2000) straight fiber pullout model was extended by adding a nonlinear spring at the end of the fiber to model the effect of mechanical anchorage. In (Georgiadi-Stefanidi, 2010) three-dimensional and simplified two-dimensional finite element model was developed to simulate the pullout of hooked-end steel fibers. In (Laranjeira, 2010) analytical model to predict the pullout response of inclined hooked-end steel fibers was proposed. The effect of the hooked-end was experimentally evaluated by subtracting the pullout curve of aligned straight fiber from the pullout curve of aligned hooked-end fiber.

The objective of this study is to derive a simple analytical model for the effect of fiber geometry on the pullout behavior of steel fibers suitable for practical use. The importance of this research lies in the fact that almost all commercially available steel fibers are mechanically deformed. The model input parameters are mechanical and geometrical properties of deformed fibers. The model is validated against experimental results on the hooked-end and crimped fiber pullout. The results show that the model is able to estimate the pullout load of mechanically deformed fibers with sufficient accuracy.

## EXPERIMENTAL: MATERIALS AND SPECIMENS

Commercially available hooked-end steel fibers HE 75/50 and HE+ 1/60 produced by ArcelorMittal were used in the pullout tests. Straight fibers were also tested to determine the bond and friction at the fiber/matrix interface. Straight fibers were obtained by cutting the hooked-ends of the HE 75/50 and HE+ 1/60 fibers. The fiber pullout specimen consisted of a single fiber embedded in a square block of cementitious matrix (see Fig. 1). The edge length of the block was 70mm. The fiber embedment length $H$ was 15mm (HE+ 1/60), 25mm (HE 75/50 fibers) and 30mm (HE+ 1/60).

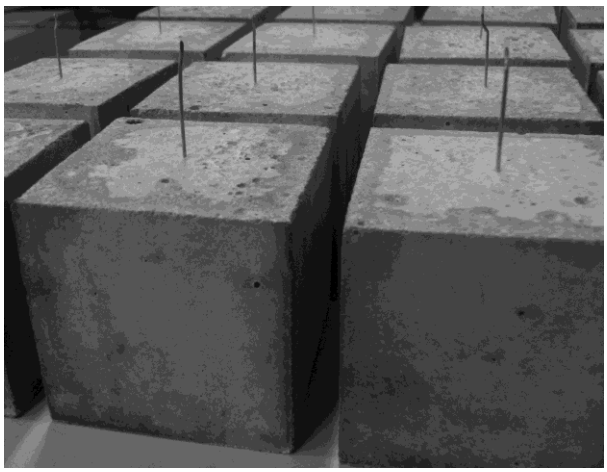

Fig. 1. Single fiber pullout specimens

To make pullout specimens, water/cement ratio of 0.5 was employed. The maximum aggregate size was 8mm. Specimens were cast in plywood molds. Oil was applied to the interior surfaces of the molds to allow easy removal of the specimens from the molds. After the casting, the molds were covered with a thin polyethylene film and left for 48 hours at room temperature. Then specimens where carefully removed from the molds and put into a water bath for further curing. After 28 days the pullout tests were carried out. The

compressive strength of the cementitious matrix was determined from three cubic specimens with an edge length of 150mm. The average compressive strength at the age of the fiber pullout tests was 39MPa. Fibers were pulled out under displacement control with a loading rate of 0.5mm/min.

Geometry of hooked-end steel fiber is shown in Fig. 2. The fiber geometry is considered as being composed of two curved segments of length $\rho\theta$ and two straight segments of length $l_e$ and $l$. The properties of the steel fibers are summarized in Table 1. The geometric parameters ($r$, $l_e$, $l$, $\rho$, $\theta$) exhibited in Table 1 were obtained by measuring specific fibers. The yield stress of steel fiber $\sigma_Y$ was taken from datasheets supplied by ArcelorMittal.

Table 1 Geometric parameters and mechanical properties of tested fibers

| **Fiber type** | $\sigma_Y$ **[MPa]** | $r$ **[mm]** | $l_e$ **[mm]** | $l$ **[mm]** | $\rho$ **[mm]** | $\theta$ **[rad]** |
|---|---|---|---|---|---|---|
| **HE 75/50** | 1100 | 0.35 | 2.00 | 2.05 | 1.73 | 0.62 |
| **HE+ 1/60** | 1450 | 0.45 | 1.89 | 1.36 | 2.23 | 0.66 |

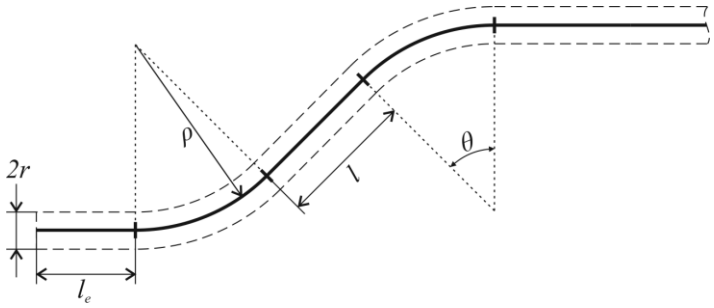


Fig. 2. Geometry of hooked steel fiber

## EXPERIMENTAL: RESULTS OF PULLOUT TESTING

Experimental pullout curves of straight steel fibers are shown in Fig. 3. After the peak load value was reached, a rapid decrease of the pullout load was observed, which corresponds to a sudden increase of damage at the fiber/matrix interface. Afterwards the pullout load nearly linearly approached zero. After debonding the pullout load is determined by the friction between the fiber and matrix.

Pullout response of hooked-end steel fibers is shown in Fig. 4. Straightening of the hooked-end and subsequent fiber pullout under frictional resistance was observed for both embedment lengths. The embedded parts of the hooked-end fibers were subjected to plastic deformations, which led to a substantial increase of the pullout resistance.

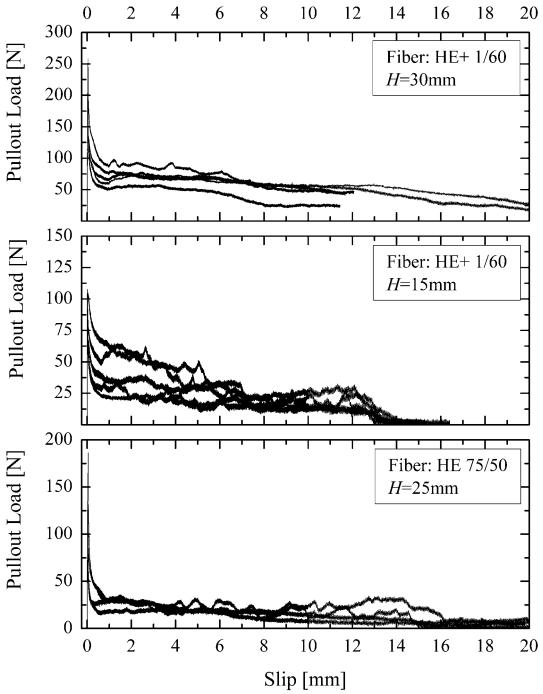


Fig. 3. Pullout response of straight steel fibers

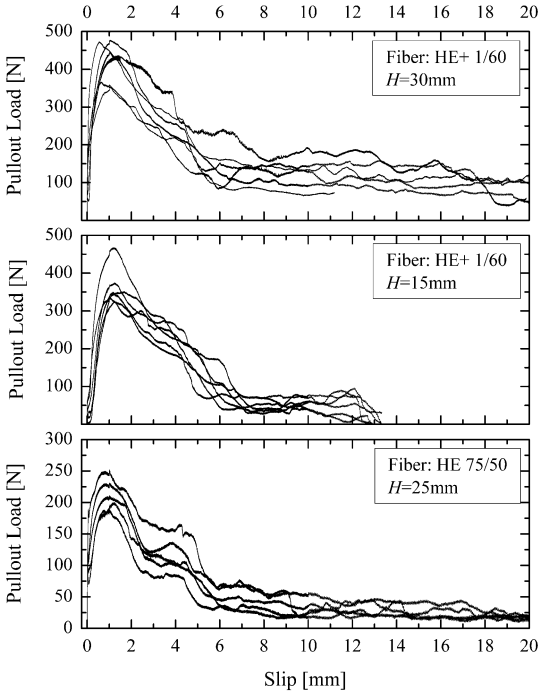


Fig. 4. Pullout response of hooked-end steel fibers

## PROPOSE MODEL: FRICTIONAL SLIDING OF FIBER THROUGH STRAIGHT MATRIX DUCT

After the fiber has fully debonded, the pullout load *P* of mechanically deformed fiber can be split into two components:

$$P = P_{pl} + P_{fric} \tag{1}$$

where $P_{pl}$ is component due to the plastic bending of the fiber in the curved matrix ducts and $P_{fric}$ is component due to the frictional sliding of fiber through straight matrix ducts. To calculate $P_{fric}$ one must determine the frictional shear stress $\tau$. The frictional shear stress can be obtained if the pullout load of straight fiber after debonding $P_s$ and the corresponding fiber slip $\Delta$ is known:

$$\tau = \frac{P_s}{2\pi r\left(H - \Delta\right)} \tag{2}$$

Fig. 5 shows averaged dependence of the frictional shear stress on the fiber slip obtained from straight fiber pullout tests (see Fig. 3). During the pullout process the frictional shear stress rapidly decreases and then remains approximately constant at a value of about 0.82MPa.

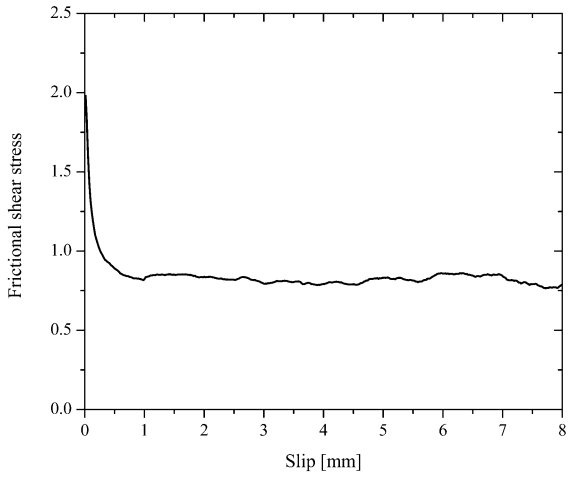


Fig. 5. Frictional shear stress as a function of fiber slip

## PROPOSED MODEL: BENDING OF FIBER UNDER TENSION

During the pullout the mechanically deformed fiber is subjected to repetitive elastoplastic bending and unbending which causes an increase of the tension in the fiber. In order to calculate $P_{anch}$, change of the tension in the fiber due to bending must be determined. The following assumptions are made:

1. The material is isotropic and strain-rate independent.

2. The Bauschinger effect is neglected during the bending and unbending.

3. The elastic strains are small in comparison with the plastic strains and can be neglected. Hence, the material is assumed to be rigid, perfectly plastic.

4. The damage of cementitious matrix around the mechanically deformed fiber during the pullout is neglected.

If the fiber is subjected to a tension force less than the yield tension $T_Y = \pi r^2 \sigma_Y$ and then to a moment sufficient to generate some curvature $\rho$, then the strain and stress distribution will be as in Fig. 6. The neutral surface will be at some distance $e$ from the mid-surface. The strain in Fig. 6 is:

$$\varepsilon_1 = \frac{e}{\rho} + \frac{x_2}{\rho} \tag{3}$$

The stress in Fig. 6 is:

$$\sigma_1 = \begin{cases} \sigma_Y, & x_2 > -e \\ -\sigma_Y, & x_2 < -e \end{cases} \tag{4}$$

The fiber tension $T$ can be expressed as:

$$T = \int_{S^-} -\sigma_Y dS + \int_{S^+} \sigma_Y dS = 2\sigma_Y \left( e\sqrt{r^2 - e^2} + r^2 \sin^{-1}\left(\frac{e}{r}\right) \right) \tag{5}$$

or

$$\frac{T}{T_Y} = \frac{2}{\pi}\left( \frac{e}{r}\sqrt{1-\left(\frac{e}{r}\right)^2} + \sin^{-1}\left(\frac{e}{r}\right) \right) \tag{6}$$

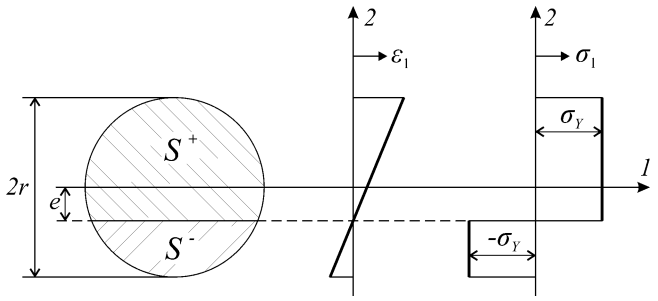


Fig. 6. Stress and strain distribution in bent plastic fiber subjected to tension

Due to the repetitive nature of bending and unbending processes the analysis may be reduced to a basic one shown Fig. 7.

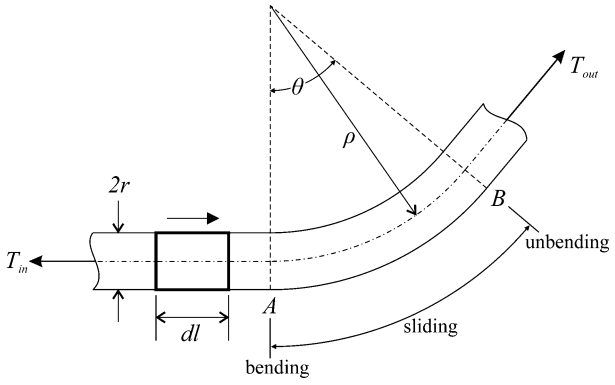


Fig. 7. Sliding of fiber element over a radius

Consider a fiber element of length *dl* which moves to the right and is bent at *A*. Then it slides against friction over the radius $\rho$ and is unbent at *B*. There are two important effects:

1. As the fiber bends at *A* and unbends at *B* there will be an increase in tension.

2. The tension will increase as the fiber slides against friction between *A* and *B*.

The plastic work done on the fiber element by deforming it at *A*:

$$W_{pl} = dl \cdot \int_S \left( \int_0^{\varepsilon_1} \sigma_1 \cdot d\varepsilon_1 \right) dS \tag{7}$$

The external work done arises from an increase of the tension $\Delta T$ at *A*:

$$W_{ext} = \Delta T \cdot dl \tag{8}$$

Then from energy balance $W_{pl} = W_{ext}$ and Eq. (3), (4), (7) and (8) we obtain:

$$\Delta T = \frac{r}{\rho}\left[ \frac{4T_Y}{3\pi}\left(1-\left(\frac{e}{r}\right)^2\right)^{3/2} + T\frac{e}{r} \right] \tag{9}$$

where *e/r* can be determined from Eq. (6). The tension in the fiber after bending at *A*:

$$T_A = T_{in} + \Delta T\big|_{T=T_{in}} \tag{10}$$

where $T_{in}$ is the tension the fiber before the curved duct *AB*.

## PROPOSED MODEL: FRICTION IN THE CURVED MATRIX DUCT

An element of length $dl=\rho d\varphi$ sliding between *A* and *B* is shown in Fig. 8. The equilibrium equation for forces in the radial direction is:

$$Td\varphi = p\rho d\varphi \tag{11}$$

or

$$p = \frac{T}{\rho} \tag{12}$$

where *p* is contact force acting on the fiber perimeter. The equilibrium equation for forces in the fiber direction is:

$$(T+dT) - T = \mu p \rho d\varphi \tag{13}$$

or by using Eq. (12)

$$\frac{dT}{T} = \mu d\varphi \tag{14}$$

where $\mu$ is coefficient of friction between the fiber and matrix. If the tension in the fiber after bending at *A* is $T_A$ (see Eq. (10)) and before unbending at *B* is $T_B$, then integrating Eq. (14) gives:

$$T_B = T_A e^{\mu\theta} \tag{15}$$

where $\theta$ is sometimes named as angle of wrap.

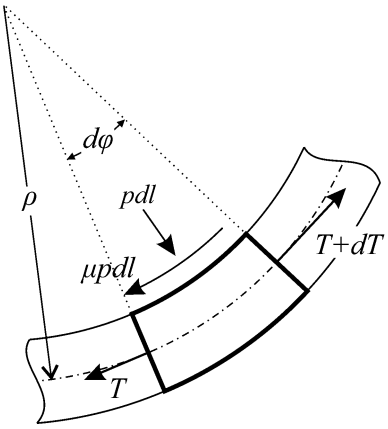


Fig. 8. Forces acting on the fiber element in the curved duct

## PROPOSED MODEL: TENSION IN THE FIBER AFTER CURVED MATRIX DUCT

During unbending at *B* there again will be an increase in tension, which can be determined from Eq. (9). Then the tension in the fiber after curved duct *AB* is:

$$T_{out} = T_B + \Delta T\big|_{T=T_B} \tag{16}$$

or

$$T_{out} = \underbrace{\left(T_{in} + \Delta T\big|_{T=T_{in}}\right)e^{\mu\theta}}_{T'} + \Delta T\big|_{T=T'} \tag{17}$$

According to Eq. (17), the tension in the fiber after *i*th curved duct is

$$T_i = \underbrace{\left(T_{i-1} + \Delta T\big|_{T=T_{i-1}}\right)e^{\mu\theta}}_{T'} + \Delta T\big|_{T=T'} \tag{18}$$

and $T_0 = 0$. During the pullout the number of curved ducts that fiber passes through gradually decreases.

## MODEL VALIDATION

The pullout process of hooked-end fiber can be divided into five stages as follows (see Fig. 9):

**Stage 1**: Fiber segments in curved ducts $C_1$ and $C_2$ subjected to plastic bending. Fiber segments in straight ducts $S_1$, $S_2$ and $S_3$ subjected to frictional sliding.

**Stage 2**: Length of the fiber segment in the curved duct $C_1$ decreases, which causes gradual reduction of pullout force component due to plastic bending. Fiber segment in curved duct $C_2$ subjected to plastic bending. Fiber segments in straight ducts $S_2$ and $S_3$ subjected to frictional sliding.

**Stage 3**: Fiber segment in curved duct $C_2$ subjected to plastic bending. Fiber segments in straight ducts $S_2$ and $S_3$ subjected to frictional sliding.

**Stage 4**: Length of the fiber segment in the curved duct $C_2$ decreases, which causes gradual reduction to zero of pullout force component due to plastic bending. Fiber segment in straight duct $S_3$ subjected to frictional sliding.

**Stage 5**: Pullout force is only due to frictional sliding of fiber segment in straight duct $S_3$.

By using Eq. (18) the pullout load $P$ as a function of fiber slip $\Delta$ in all stages can be written as follows:

$$P=\begin{cases} T_2+2\tau\pi r\left(H_s+l+l_e-\Delta\right), & \Delta\le l_e \\ T_2+\dfrac{T_1-T_2}{\rho\theta}\left(\Delta-l_e\right)+2\tau\pi r\left(H_s+l\right), & l_e<\Delta\le l_e+\rho\theta \\ T_1+2\tau\pi r\left(H_s+l+l_e+\rho\theta-\Delta\right), & l_e+\rho\theta<\Delta\le l_e+l+\rho\theta \\ T_1\left(2-\dfrac{\Delta-l_e-l}{\rho\theta}\right)+2\tau\pi rH_s, & l_e+l+\rho\theta<\Delta\le l_e+l+2\rho\theta \\ 2\tau\pi r\left(H_s+l+l_e+2\rho\theta-\Delta\right), & l_e+l+2\rho\theta<\Delta\le l_e+l+2\rho\theta+H_s \end{cases} \tag{19}$$

where $H_s=H-l_e-l\cos\theta-2\rho\sin\theta$ is length of embedded part of the fiber without hook before pullout process. For the sake of simplicity, it is assumed that the component of pullout load due to plastic bending decreases linearly when the fiber end passes through curved duct.

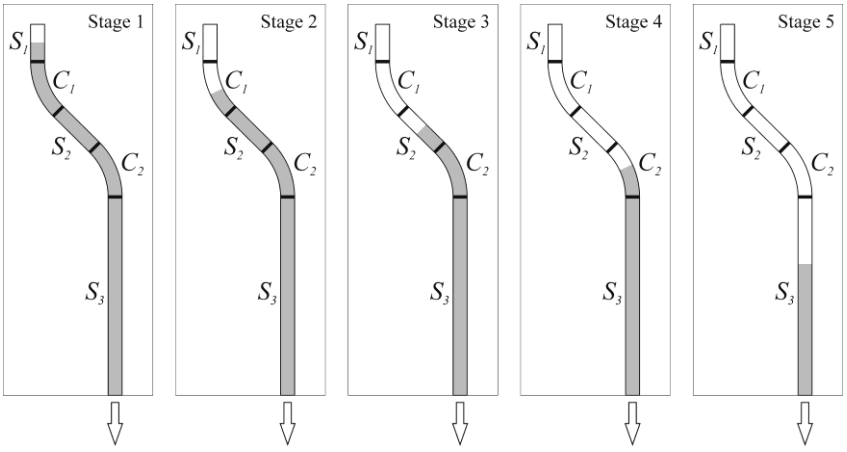


Fig. 9. Schematic diagram of hooked fiber pullout

Enlarged initial portion of typical experimental pullout curve of hooked fiber is shown in Fig. 10. Debonding along the fiber/matrix interface occurs when the pullout load reaches $P_d$. Experimentally there is a sudden load drop after $P_d$. Then pullout load starts to increase again until it reaches $P_{pb}$ and the reaction force acting on the curved fiber segments is sufficient to initiate plastic bending of the fiber. At this point the fiber slip is approximately 0.5-1mm. It can be seen from Fig. 6 that at the initiation of plastic bending the frictional shear stress has decreased to approximately 0.82MPa. Since this model focuses on the calculation of pullout load, when the hooked-end is fully mobilized, then $\tau$ =0.82MPa will be used in Eq. (19).

It was postulated in (Geng, 1997) that there exists one-to-one relationship between the coefficient of friction $\mu$ and frictional shear stress $\tau$ after debonding is completed. This can be explained by the fact that both $\mu$ and $\tau$ are dependent on the current status of the interface.

Based on the experimental data, the following empirical relation between both parameters was proposed in (Geng, 1997):

$$\mu = \mu' + \frac{\tau}{\tau'} \tag{20}$$

where $\mu' = 0.08$ and $\tau' = 21.28\text{MPa}$ . From Eq. (20) follows that if $\tau$ =0.82MPa then $\mu$=0.12, which will be then used for the coefficient of friction in Eq. (18).

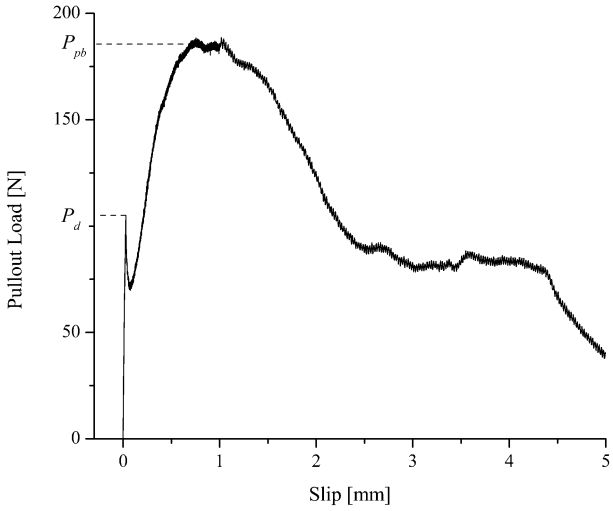


Fig. 10. Initial portion of typical experimental pullout curve of hooked fiber

Modeling results obtained using Eq. (19) are shown in Fig. 11. Satisfactory correlation can be observed between the predicted and experimental pullout curves. The experimental pullout load during purely frictional phase is higher due to incomplete straightening of the hooked-end which is not taken into account in this model.

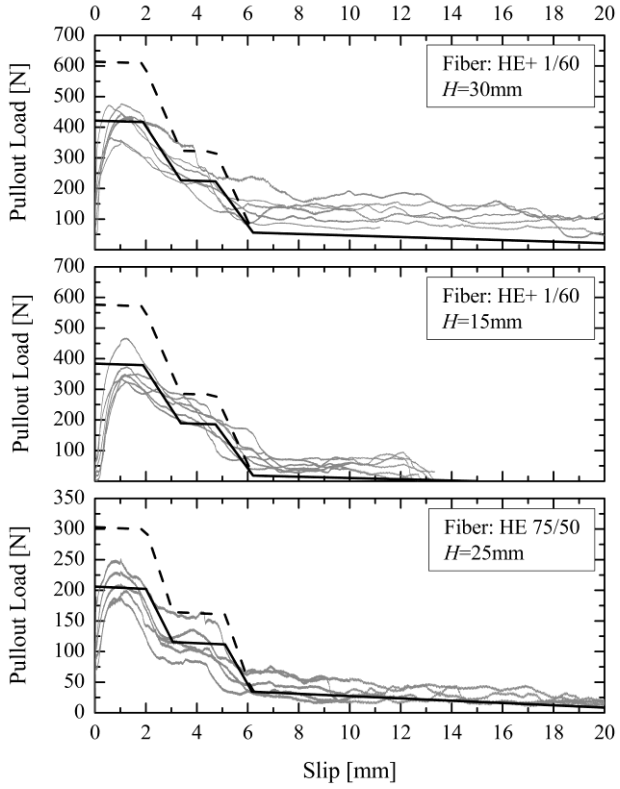


Fig. 11. Validation of the proposed model (black line) against experimental data (gray lines) for hooked-end fibers. Dashed line – prediction of the frictional pulley model (Alwan, 1999)

For comparison, predictions of the frictional pulley model (Alwan, 1999) are also presented in Fig. 11. Details of the frictional pulley model can be found in Appendix A. It can be seen that the frictional pulley model heavily overestimates the hooked-end contribution. This can be explained by the fact that frictional pulley model does not take into account the curvature of the curved duct $1/\rho$, which influences the amount plastic work required to straighten the fiber.

## CONCLUSIONS

A simple model is developed to simulate the mechanical contribution of fiber geometry to the pullout response. It is assumed that fiber geometry is composed of straight and curved segments. The mechanical contribution depends on the amount of plastic work required to straighten the fiber during pullout and friction in the curved ducts. The plastic work is a function of geometrical parameters and yield stress of the fiber. The damage of cementitious matrix during pullout is neglected.

The model provides a reasonably good description of experimental pullout data of crimped and hooked-end steel fibers. Besides, the model is able to predict fiber failure due to breaking.

## ACKNOWLEDGMENTS

This work has been funded by ERAF via project 2010/0293/2DP/2.1.1.1.0/10/ APIA/VIAA/073.

## APPENDIX A. FRICTIONAL PULLEY MODEL

The frictional pulley model for hooked-end steel fibers was developed by (Alwan, 1999). Sketch of the frictional pulley model is shown in Fig. A.1. The model consists of two frictional pulleys. Both pulleys have rotational and tangential components of friction resisting the pullout process. The rotational friction component corresponds to the work needed for straightening the steel fiber. The tangential friction component represents the friction between the steel fiber and matrix in the curved duct. The pullout load due to mechanical anchorage when fiber passes through two curved ducts is given as:

$$T_2 = \frac{T_Y}{3\cos\alpha\left(1-\mu\cos\beta\right)}\left(1+\frac{\mu\cos\beta}{1-\mu\cos\beta}\right)$$

If fiber passes through one curved duct, then:

$$T_1 = \frac{T_Y}{6\cos\alpha\left(1-\mu\cos\beta\right)}$$

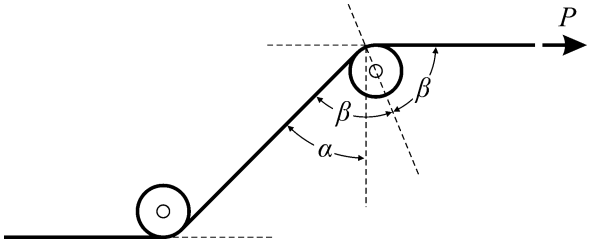


Fig. A.1. Frictional pulley model (Alwan, 1999)

## REFERENCES

Alwan JM, Naaman AE, Guerrero P. Effect of mechanical clamping on the pull-out response of hooked steel fibers embedded in cementitious matrices. Concrete Science and Engineering, 1999, 1, p. 15-25.

Alwan JM, Naaman AE, Hansen W. Pull-out work of steel fibers from cementitious composites: Analytical investigation. Cement and Concrete Composites, 1991, 13, p. 247-255.

Banthia N, Trottier JF. Concrete Reinforced with Deformed Steel Fibers, Part I: Bond-Slip Mechanisms. ACI Materials Journal, 1994, 91, p. 435-446.

Chanvillard G, Modeling the pullout of wire-drawn steel fibers. Cement and Concrete Research, 1999, 29, p. 1027-1037.

Cunha VMCF, Barros JAO, Sena-Cruz JM. Pullout Behavior of Steel Fibers in Self-Compacting Concrete. Journal of Materials in Civil Engineering, 2010, 22, p. 1-9.

Geng YP, Leung CKY. Damage-based modeling of fiber pullout under variable compressive stress. Journal of Engineering Mechanics, 1997, 123, p. 342-349.

Georgiadi-Stefanidi K, Mistakidis E, Pantousa D, Zygomalas M. Numerical modelling of the pull-out of hooked steel fibres from high-strength cementitious matrix, supplemented by experimental results. Construction and Building Materials, 2010, 24, p. 2489-2506.

Laranjeira F, Aguado A, Molins C. Predicting the pullout response of inclined straight steel fibers. Materials and Structures, 2009, 43, p. 875-895.

Laranjeira F, Molins C, Aguado A. Predicting the pullout response of inclined hooked steel fibers. Cement and Concrete Research, 2010, 40, p. 1471-1487.

Lee Y, Kang ST, Kim JK. Pullout behavior of inclined steel fiber in an ultra-high strength cementitious matrix. Construction and Building Materials, 2010, 24, p. 2030-2041.

Leung CKY, Shapiro N. Optimal Steel Fiber Strength for Reinforcement of Cementitious Materials. Journal of Materials in Civil Engineering, 1999, 11, p. 116-123.

Naaman AE, Namur GG, Alwan JM, Najm HS. Fiber Pullout and Bond Slip. I: Analytical Study. Journal of Structural Engineering, 1991a, 117, p. 2769-2790.

Naaman AE, Namur GG, Alwan JM, Najm HS. Fiber Pullout and Bond Slip. II: Experimental Validation. Journal of Structural Engineering, 1991b, 117, p. 2791-2800.

Robins P, Austin S, Jones P. Pull-out behaviour of hooked steel fibres. Materials and Structures, 2002, 35, p. 434-442.

Sujivorakul C, Waas AM. Pullout response of a smooth fiber with an end anchorage. Journal of Engineering Mechanics, 2000, 126, p. 986-993.